International Journal of Current Engineering and Technology
E-ISSN 2277 – 4106, P-ISSN 2347 – 5161

Available at http://inpressco.com/category/ijcet

Research Article

Fault-Tolerant Position Control of the Manipulator of *PUMA* Robot using Hybrid Control Approach

Seema Mittal †, M.P. Dave ‡ and Anil Kumar †

†Ajay Kumar Garg Engineering College, Ghaziabad, India
‡Dept. Electrical Engineering, Shiv Nader University, NCR Delhi, India
†Al Falah University, Dhauj, Faridabad, India

Accepted 17 Oct 2016, Available online 19 Oct 2016, **Vol.6, No.5 (Oct 2016)**

Abstract

The position control of a standard robotic arm under faults has been studied and the performance is compared using a combination of several control approaches. The manipulator of a robot is exposed to possible faults and combinations of control techniques are employed. Here, several control combinations of PID along with optimal and robust techniques such as LQR, H_2, H_∞ and H_∞-static output feedback (SOPF) controls have been designed. The control gains have been obtained offline using equivalent linearization of the robot dynamic system. The hybrid controls are implemented online on PUMA 560 robot. The relative efficiency has been obtained using H_2- control augmented with PID. The proposed hybrid control approach has been successfully implemented on six degree of freedom robot accommodating common types of faults represented as an exponential function, sudden or abrupt in nature.

Keywords: *Fault-tolerant control, PUMA robot, hybrid control, PID, LQR, H_2 control, H_∞ control, performance of robot.*

1. Introduction

Robots have been used widely in industry or in health or other services for mankind. An important component of the robotic arm is precise placement of the target in space. The inherent uncertainties associated with the modeling of the robot warrants considerations of non-linearity. The electro-mechanical devices of the robot may also develop faults in any of its component thus affecting the normal functioning of the system. Therefore, an appropriate control technique is a critical component of the functioning of robots (Vemuri, 1997; Acosta *et al*, 1999; Gao *et al*, 2015).

In a complex situation particularly, under influence of coupling among different terms in equation of motion i.e. rotation of one joint affects motion of other joints, it may be desirable to employ a combination of different control techniques. As noted by Pawar (2016), Proportional-integral-derivative (PID) based control technique may not yield optimal control results. He employed a combination of PI and fuzzy controller and demonstrated its efficacy in the induction motor system. Hossam (2014) utilized a combination of the nominal feedback controller along with a variable structure compensator for tracking control of a two-link robot manipulator.

Attempts have been made to utilize linearized models by several authors such as Levi *et al*, 2007 who studied the tracking problem of a robotic system by solving Nonlinear Hamilton-Jacobi Inequality (HJI) using Linear Matrix Inequalities (LMIs), with external disturbance and model uncertainties. They designed the controller using linear $H\infty$ control by transforming the nonlinear model as a linear system. The technique was demonstrated on a two-link manipulator with known model properties.

Using a feedback linearization Lofti *et al* (2010) have designed a controller for an electro-pneumatic cylinder for application in parallel robots. The proposed controller consists of Generalized Predictive Controller (GPC) which was used for the position of outer loop and a constrained based LMI for H_∞ controller for the pressure inner loop. Here, the use of predictive theory was useful as the future trajectory was known a priori since the trajectories are preplanned. Good performance in terms of robustness and dynamic tracking was recorded experimentally on Adept Quattro system. Ruby Meena *et al* (2015) have reported results using PID controller having single or two degrees of freedom (DOF) which was tuned using genetic algorithm (GA) and employed in a reheat thermal system. They observed that two-DOF PID controller provided improved transient responses.

Gadewadikar *et. al* (2009) have proposed a new algorithm for obtaining H_∞-static output feedback

*Correspondiung author **Seema Mittal** is working as Assistant Professor**, M.P. Dave** as Visiting Professor **and Anil Kumar** as Professor

(SOPF) by solving only two Ricatti equations instead of three. They observed while working with the control of F16 aircraft that H_∞-SOPF provided better results than optimal feedback control (OPFB) particularly when disturbances exist in the system.

In the present study, the control of the manipulator of a standard robot PUMA 560 has been implemented using various control techniques e.g. PID, LQR, H_2, H_∞ and a recently proposed H_∞-static output feedback (SOPF) control methodology. It may be noted that a single control technique has not been able to provide desired solutions under such a complex situation. Therefore, a combination of different control approaches has been employed. The control parameters have been computed offline using a linearized state space formulation and implemented online on the robot. The proposed methodology helps to achieve positioning the arm at the target more efficiently. The optimum position control of the robotic arm has been achieved which has a practical significance for an optimum utilization of the robot.

2. Description of PUMA Robot

2.1 Engineering Parameters of Robot

PUMA 560 is a standard robot having six-degrees of freedom system. It consists of six arms called links and connecting them are six joints. Further, the first three joints are called as shoulder, elbow and wrist joints as shown in Figure 1 (adapted from Rutherford). The joints 4, 5 and 6 help achieving proper orientation of the end effector to hold an object in a desired manner.

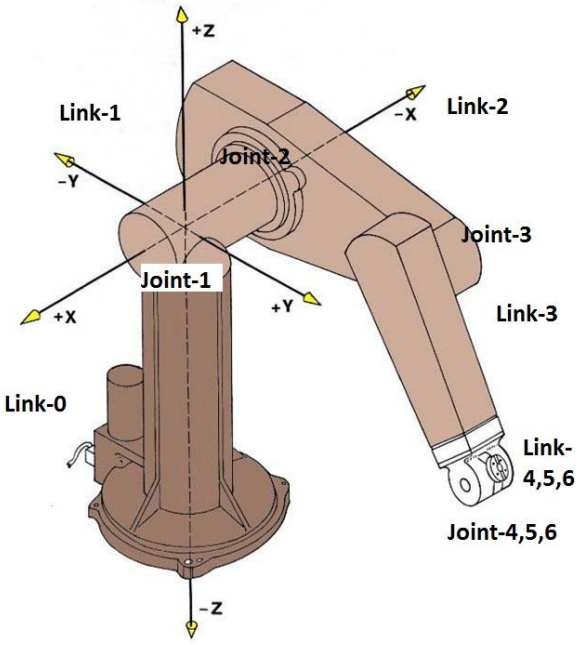

Fig.1 Schematic of Puma Robot

The engineering parameters of the standard PUMA 560 robot have been considered as provided by Corke *et al* (1994). The assessment of parameters of the robot manipulator remains a continuous effort (Yan *et al*, 2015). The actuator's physical limits i.e. the response of motors can be considered as the bounds imposed by capacity of the actuators and are provided in Table 1.

Table 1 Actuator Physical Limits

Parameter for Motor	Type of Motor					
	PR 090	PR 090	PR 090	PR 070	PW 0701	PW 0702
Rotation (degree)	±320	±250	±270	±300	±200	±532
Velocity (deg/sec)	149	149	149	149	248	320
Acceler-ation (deg/sec^2)	596	596	596	596	992	1280
Current (Amp@ 24V)	30	30	30	15	15	15
Output torque (Nm)	206	206	206	73	54	28
Used in joint	1	2	3	4	5	6

2.2 Dynamic Modeling and Equivalent Linearization of Robot Manipulator

Considering the geometric and other parameters, the dynamic equation of motion of the robot can be expressed as in Equation 1.

$$M\ddot{q} + Vm(q,\dot{q})\dot{q} + \mathcal{G}(q) + F(\dot{q}) = \tau \qquad (1)$$

Here, $q = [q_1, q_2, q_3, q_4, q_5, q_6] \in \mathcal{R}^n$ are the joint positions $(n = 6)$ equal to the d.o.f. of the robot system, $M(q) \in \mathcal{R}^{nxn}$ is the inertia matrix and is symmetric positive definite, $Vm(q, \dot{q}) \in \mathcal{R}^{nxn}$ represents Coriolis and centripetal forces, $F(\dot{q}) \in \mathcal{R}^n$ is the dynamic frictional force matrix, $\mathcal{G}(q) \in \mathcal{R}^n$ is the gravity matrix and τ denotes generalized input control of the system applied at the joints. The simulation of functional aspects of the PUMA 560 robot such as kinematics, dynamics and trajectory generation have been carried out using Robotics Toolbox (Corke, 2011) with some modifications. This has been used to generate responses namely $q, \dot{q}, \ddot{q}$ by solving dynamic equations of motion (without friction) using recursive Newton Euler (RNE) method.

The complexities in the modeling may be appreciated by observing variation in inertia or the control gains required during motion of the arm. The control gains at various positions of the joint angles (by varying values of q_2, q_3) have been computed and its variation has been shown in Figure 3.

A linear model of PUMA 560 as proposed by Clover (1996) has been adopted in the present study. The suggested linearization of nonlinear dynamic equations uses the Taylor series expansion of nonlinear functions about a nominal trajectory after neglecting higher order terms (retaining first order term) and are expressed for a function, f as follows.

$f(q, \dot{q}, \ddot{q})=$

$$f(q^*, \dot{q}^*, \ddot{q}^*)+\left\{\frac{\partial f}{\partial q}\Big|_{q^*}\right\}\delta q+\left\{\frac{\partial f}{\partial \dot{q}}\Big|_{\dot{q}^*}\right\}\delta \dot{q}+\left\{\frac{\partial f}{\partial \ddot{q}}\Big|_{\ddot{q}^*}\right\}\delta \ddot{q} \quad (2)$$

The Equation-2 can also be written in a linear form as given in Equation-3 as applicable to the robot dynamics.

$$\delta\tau = M_0(q^*)\,\delta\ddot{q} + C_0(q^*, \dot{q}^*)\,\delta\dot{q} + K_0(q^*, \dot{q}^*, \ddot{q}^*)\,\delta q \quad (3)$$

Here q^* denotes the nominal trajectory, $M_0, C_0, K_0 \in \mathcal{R}^{nxn}$ linearized trajectory sensitivity matrices in terms of the nominal trajectory. The Equation-3 can be formulated in to state space form as shown in Equation-4.

$$\frac{d}{dt}\begin{bmatrix}\partial q \\ \partial \dot{q}\end{bmatrix} = \begin{bmatrix}0 & I \\ -M_0^{-1}K_0 & -M_0^{-1}C_0\end{bmatrix}\begin{pmatrix}\delta q \\ \delta \dot{q}\end{pmatrix} + \begin{bmatrix}0 \\ -M_0^{-1}\end{bmatrix}(\delta\tau). \quad (4)$$

The standard state space form as given below is adopted, where, $x(t)$ is the state vector consisting of $[q\ \dot{q}]^T \in \mathcal{R}^{2n}$. The input control vector is $u(t) \in \mathcal{R}^n$, $y(t) \in \mathcal{R}^{2n}$ is the output vector and $C(t) \in \mathcal{R}^{2nx2n}$ is the output matrix.

$$\dot{x} = A(t)x(t) + B(t)u(t) \text{ and } y = C(t)x(t) + D(t) \quad (5)$$

The matrices of the state space system (G) as depicted in Figure 2 constitutes matrices $A(t), B(t), C(t), D(t)$ and can be expressed as given below.

$$A = \begin{bmatrix}0 & I \\ -M_0^{-1}K_0 & -M_0^{-1}C_0\end{bmatrix};\ B = \begin{bmatrix}0 \\ -M_0^{-1}\end{bmatrix};$$

C(t) = diag ([1,1,1,1,1,1]) and D(t)=[0]. (6)

The values of state space matrices and other relevant details may be referred to Mittal *et al*, 2016.

3. Modeling Faults

The control scheme should be able to accommodate uncertainties arose from modeling geometry and elastic parameters of the robot as well as some of the possible types of faults. The present study considers the failure of actuators only. The value of states of robotic parameters are assumed to be bounded and are expressed as $q(t)$, $\dot{q}$(t) ϵ L∞, here L∞ being some bound. Also, the uncertainties due to faults are considered to be finite in magnitude.

For simulation, the trajectory to be simulated in terms of q vector is from an initial point described by $q_{1i}\ in\ radians$ = (1, 1, 1, 1, 1, 1), for $i = 1\ to\ 6$, to a target point q_{2i} (1.5, 3, 4, 1.5, 1.5, 1.5) and allowing rotations of all the six joints in the system. The desired trajectory (q_d) is a seventh degree polynomial fitted between the mentioned two points at a time step (Δt) of 0.056 seconds. In the present simulations, three types of actuator faults or disturbance mentioned as below are studied.

Case 1. Lock-in fault in actuator

The actuator failure (the motor thus affects the constrained rotation of the concerned joint) takes place at a joint in which a constant torque is exerted on the system such as at q_2, the torque $\tau_2 = -40$, for an interval of $1.5 \le t \ge 2.5$ seconds. Similar type of fault was simulated successfully at other joints.

Case 2. Sinusoidal actuator failure

In this case, the faulty actuator imposes sinusoidal type of torque representing a time varying actuation (Rugthum and Tao, 2015) at joint-2 described as, $\tau_2 = -40\sin(0.3t)$, for the interval $1.5 \le t \ge 2.5$ seconds.

Case 3. Exponential actuator failure

In this case, the faulty actuator imposes exponential type of torque representing a time varying actuation at joint-2 described as, $\tau_2 = -40e^{-0.5t}$, for the interval $1.5 \le t \ge 2.5$ seconds.

4.0 Controlling of Robot System

4.1 Design of Controller

The controllers using close loop feedback control system as shown in figure-2 are designed for a standard PUMA 560 robot for positioning the end effector.

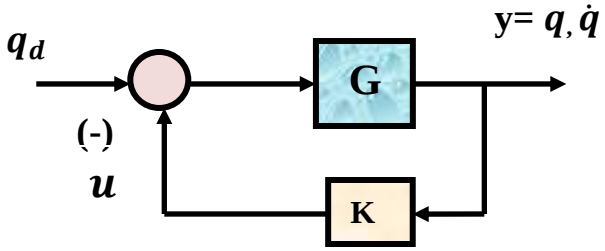

Figure 2 Feedback control of the system *G*

The following assumptions regarding the modeling are considered.

i) The initial state of the system $x(0)$ is available.
ii) The system states $q, \dot{q}$ remains bounded even after occurrence of a fault such that $\{q, \dot{q}\} \in \Omega_q$, where Ω_q is the (finite) region of operation.
iii) The capacity of the load (load disturbance) is bound such that the desired (nominal) torque $\|\tau_d\| \le \tau_m$ remains within certain bounds which may be interpreted as load carrying capacity of the robot (τ_m) and its value is known. The tracking error is defined as $e(t) = q_d(t) - q(t)$, and $\dot{e} = (\dot{q}_d - \dot{q})$, here $q_d(t)$ is the desired trajectory. Based on this formulation, the control is designed offline by getting K_{gains} from a particular technique. These gains are adopted to provide control input torque to

the robot system online simulating a predefined trajectory of the end effector. The considered control techniques are described in the next section.

4.2 Proportional–Integral–Derivative Controller (PID)

In the feedback control mechanism, the part of the output is fed into the system so that the errors get reduced. The plant having input *'u'* and output *'y'* is described by the model *'G'* and the gain by *'K'* (Figure-2). An error vector is computed by comparing the observed output and the desired output of joint rotations. The parameters in PID controller are chosen such that the error, $e(t)$ gets vanish in certain finite time. In general, there are three components of a PID controller namely proportional, integral and derivative terms. These terms consist of coefficients denoted as K_P, K_I *and* K_D which when multiplied with the error term, integral of error and the derivative term of the error respectively, give feedback gain to the system to be controlled. The feed gain matrix of PID in time domain is expressed as in Equation 7.

$$\boldsymbol{u(t) = K_P\, e(t) + K_I \int_0^t e(t)dt + K_D \frac{d\, e(t)}{dt}} \qquad (7)$$

The following values of the three components of PID have been arrived at by trial and error for accommodating even fault condition;

$K_P = (450, 1200, 200, 120, 120, 120),$
$K_I = (300, 1200, 50000, 500, 500, 500),$
$K_D = (-20, -200, -20, -50, -50, -50).$

4.3 Linear Quadratic Regulator (LQR)

Another control technique called Linear Quadratic Regulator (LQR) is used in which closed loop poles are decided not arbitrarily but by optimizing a performance index (J). Therefore, this control is an optimal type and the required control energy is given in Equation 8.

$$J = \int_0^\infty (x^T Q\, x + u^T R\, u)dt \qquad (8)$$

Here, Q is a positive definite or positive semi-definite Hermitian or real symmetric matrix and is called the state-cost weighted matrix. R is a positive definite or a real symmetric matrix and is called the control weighted matrix (Ogata, 2012). The second term of J represents an expenditure of energy of the control signal and is related to the energy requirement by the actuator. The process involves solving algebraic Riccati equations (ARE) to obtain gains, K_{gain} and the state feedback control input, $u = -K_{gain}x$ is applied. This ensures that the closed loop system ($A_C = A - BK_{gain}$) is asymptotically stable. The resulting poles are shown in Figure 6. Using state space form described in equation 6, the control gains are computed by choosing appropriate Q and R. Further, to highlight the magnitude of nonlinearity in the system the norm of the control gain is computed for a combination of various q_i ($q_1 = 1,\ -\pi \le q_2 \le \pi,\ -\pi \le q_3 \le \pi$) for certain Q and R and its variation is shown in Figure 3.

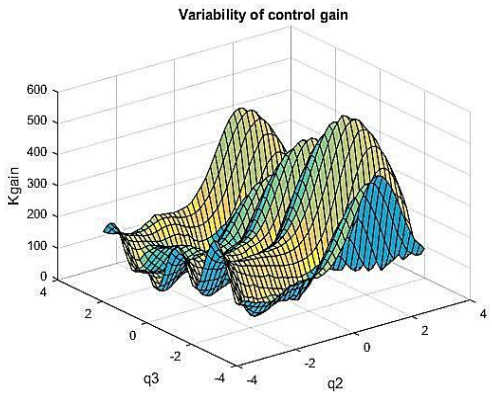

Figure 3 Variability of norm of control gain using LQR for a range of q

4.4 H_2- Feedback Control

The output feedback using H_2- Control is a robust control and can be described by the block diagram as shown in Figure 4. Here, G is the system to be controlled, K is the desired optimal control gain which stabilizes the closed loop system.

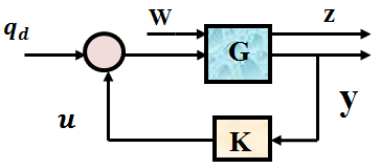

Figure 4A Schematic of H_2- control

The problem of control process becomes to minimize H_2-norm of the transfer matrix T_{zw} from w *to* z. The state model of G *and* K are used so that state reaches zero from all initial values when $w = 0$, called internal stability. Here, w is the disturbance function, z is the controlled output to be minimized and y is the measurand output. The system G is partitioned as given in Equation 9 and is expressed in the state space form in Equation 10.

A 12x12	B1 12x 6	B2 12x6
C1 6x12	D11 6x6	D12 6x6
C2 6x12	D21 6x6	D22 6x6

Figure 4B Partition sizes of matrices in H_2 or $H\infty$ control

The adopted sizes of matrices in H_2 or H∞ control are indicated in Figure 4B.

$$G = \left[\begin{array}{c|cc} A & B_1 & B_2 \\ \hline C_1 & D_{11} & D_{12} \\ C_2 & D_{21} & D_{22} \end{array}\right] \quad (9)$$

$$\begin{aligned} \dot{x} &= Ax + B_1 w + B_2 u, \\ z &= C_1 x + D_{11} w + D_{12} u, \\ y &= C_2 x + D_{21} w + D_{22} u \end{aligned} \quad (10)$$

Here, input to $B_1$are the disturbances, input to B_2 are the control input, output of C_1 are the errors to be minimized and output of C_2 are the output measurements provided to the controller. The norm of the matrix G relates to frequency domain and the cost γ of the transfer matrix ($\|T_{zw}\|^2$) is optimized (Doyle *et al*, 1989). The associated Hamiltonian matrices H_2 *and* J_2 are constructed which belong to an appropriate Riccati domain. For numerical consistencies, the matrices $D_{11} = D_{22} = 0$. The H_2 optimal gain is computed using MATLAB toolbox and the control input as $u = Ky$ is applied to the system. This control gain has been found to be insufficient to achieve the desired position of the end effector when the fault as mentioned in Section 3 is introduced in the system. the resulting trajectory which, has large steady error for all the six joints is shown in Figure 5. However, a combination of this gain along with from other techniques (PID) has been attempted whose details are provided in the next section.

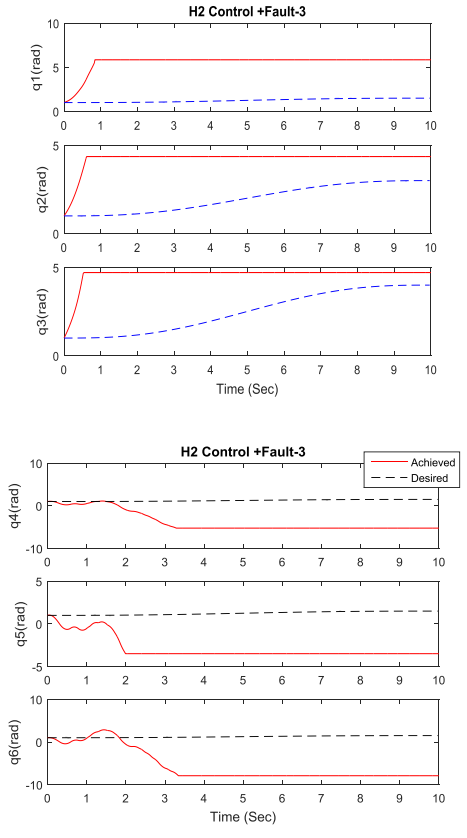

Figure 5 Response of H_2 control without PID

4.5 H∞- Feedback Control

Similar to H_2 control, the norm of matrix G relates to frequency domain in the H_∞ control and the optimal cost is minimized relative to γ, a positive value so that the norm of the transfer function satisfies a condition $\|T_{zw}\|_\infty < \gamma$, as given in Equation 11.

$$\|T_{zw}\|^\infty \triangleq \frac{sup}{\omega} \sigma_{max}\left(T_{zw}(j\omega)\right) < \gamma \quad (11)$$

Detailed description and process of H_∞ control may be referred in Gahinet and Apkarian, 1994; Zhou, 1992. One of the major difference between H_2 and H_∞ controls is that the optimal K_∞ controller is difficult to characterize compared to sub-optimal ones. The H_∞ controller relates the optimum gain in the presence of the "worst case" disturbance (w_{worst}). The spectral radius of (X_∞,Y_∞) must be less than or equal to γ^2. The control gain is obtained for the system as described in Equation 12.

It has been observed after simulations that similar to H_2 control the obtained gain is not sufficient to achieve the position of the end effectors and further results are discussed in the Section 5.

4.6 H∞-Static Output Feed Back Control

Another control technique using H∞-Static Output Feed Back *(SOPF)* has been proposed by Gadewadikar *et al*, 2009 which is relatively simpler in implementation and is described below.

$$\dot{x} = Ax + Bu + Dd, \text{and } y = Cx \quad (12)$$

The performance output ($\|z(t)\|^2$) is also defined similar to J in Equation 8. The matrices are standard state space matrices, $d(t)$ is disturbance input matrix. Q and R are positive matrices and C is of full row rank matrix. The system $\mathcal{L}_2$ gain will be attenuated by γ if the condition given by Equation 13 is satisfied. The value of γ should be bounded by a predefined minimum γ^* (i.e. $\gamma > \gamma^*$).

$$\frac{\int_0^\infty \|z(t)\|^2\, dt}{\int_0^\infty \|d(t)\|^2\, dt} = \frac{\int_0^\infty (x^T Q\, x + u^T R\, u) dt}{\int_0^\infty (d^T Q\, d) dt} \leq \gamma^2 \quad (13)$$

The constant state feedback gain is defined as $u = -K_s x$. The process is iterative where coupled equations are solved for state feedback. An initial state-variable feedback (SVFB) gain is calculated (using other standard control approach such as LQR) and is projected onto null space perpendicular to C. The algorithm is summarized as below.

Step-1, Initialize: Fix $\gamma > \gamma^*$. Set n=0, $L_0 = 0$. Calculate initial gain K_{s0} and closed loop matrix, $A_0 = A - BK_{s0}$. Assume appropriate matrices for Q and R, which may be scaled for convergence as reported by Gadewadikar*et al*. In the present study, Q and R matrices are diagonal unit matrices.

Step-2, n-*th* iteration: Solve ARE for P given by Equation 14,

$$P_n(A_n) + (A_n^T)P_n + Q + K_{sn}^T R K_{sn} + \frac{1}{\gamma^2} P_n D D^T P_n = 0 \quad (14)$$

Next is to update K_{sn} *and* L_n. The singular value decomposition (SVD) of C matrix is computed whose components are used as $= USV^T = U[S_0 \quad 0]\begin{bmatrix} V_1^T \\ V_2^T \end{bmatrix}$.

Using $K_{s(n+1)} = R^{-1}(B^T P_n + L_n)(I - V_2 V_2^T)$.
$L_{n+1} = RK_{sn} - B^T P_n$. and $A_{n+1} = A - BK_{s(n+1)}$.
Step-3, Check convergence: When converged which can be checked using the norm of $P_{n+1} - P_n$, go to the next step otherwise set $n = n + 1$ and go to step-2.
Step-4, End. Set $K_s = K_{s(n+1)}$ and compute OPFB gain using $K = K_s V_1 (S_0^{-1}) U^T$.

For the present study, it has been observed that the control gain as obtained during various iterations fluctuates between the gain of LQR and of **H∞** control.

5. Hybrid Control of Faults

The complexities grow more noting that there may not be prior knowledge of the type of fault for which controller is to be designed. Several researchers have implemented the fault control scheme in more than one stage because a single controller may not yield desired results, as noted by Lei and Meng, 2004; Sunan and Tan (2008) and others. Sunan and Tan (2008) have used two artificial neuron network (ANN) controllers in which the second ANN improves the performance after getting information about the fault from the first ANN. Using PID controller, Tihomir *et al* (2012) have observed that it was not possible to asymptotically track the position reference trajectory varying with time.

It may be noted that several researchers have implemented their suggested control methodology on a two-link (joints) system. However, in the presently studied system, there are six-links/ joints and the model incorporate the features of kinematics and dynamics simulation thus simulating practical situations.

The poles (eigen values) as obtained in different control techniques are plotted in Figure 6. The poles of the matrix, A which represents an unstable system have positive real component (in the range of +0.85±2.91 to -0.227±1.83 and zero values). It may be observed that the poles of the controlled systems lie in the left half plane suggesting that the designed system should yield stable controls. The range in terms of the maximum and the minimum values of poles are in case of LQR as (-9.11, -0.117±5.15, and zero values), for H_2 control as (-0.89±2.09 and -0.002+3.03), and for H_∞ control as (-0.89±2.09 and -0.189±3.03).

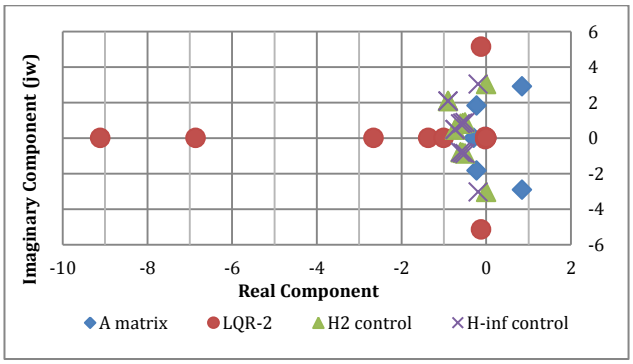

Figure 6 Observed location of poles for different controls

The H_2 control signal is given by $= -K_2 x$. The gain matrix K_2 consists of two components corresponding to two components of the vector x i.e. q and $\dot{q}$ as

$$K_2 = [K_{2e}, K_{2ed}]. \quad (15)$$

The values of the gain components and coefficients of PID are given below for hybrid H_2 control.

K_{2e}=

-4.3278	-0.2105	-0.1314	0	0	0;
-0.1878	-4.5059	-0.3861	0	0	0;
-0.1295	-0.3692	-1.1626	0	0	0;
0	0	0	-0.2000	0	0;
0	0	0	0	-0.1800	0;
0	0	0	0	0	-0.1900];

K_{2ed}=

-6.4949	-0.2706	-0.1669	0	0	0;
-0.2887	-6.2951	-0.4863	0	0	0;
-0.1947	-0.5218	-1.5095	0	0	0;
0	0	0	-0.2400	0	0;
0	0	0	0	-0.1980	0;
0	0	0	0	0	-0.1900];

The values of coefficients of PID as per section 4.2 are diagonal matrices as given below.
$K_{2P} = (0)$,
$K_{2I} = diag([-4000, -10000, -5600, -1900, -2900, -1000])$,
$K_{2D} = diag([-110, -200, -20, -20, -20, -20])$.

Further, the H_∞ control signal is given by $= -K_\infty x$ and the gain matrix K_∞ consists of two components defined by Equation 15. The values of the gain components and coefficients of PID are given below for hybrid H_∞ control.

$K_{\infty e}$=

-4.3197	-1.4589	-0.2205	0	0	0;
-0.0488	-6.0453	-1.2843	0	-0.0001	0;
-0.1042	-0.2828	-1.3149	0	0	0;
0	0	0	-0.2000	0	0;
0	0	0	0	-0.1800	0;
0	0	0	0	0	-0.1900];

K∞ed=

```
[ -6.6767  -0.5419  -0.0438       0       0       0;
  -0.5052  -7.5408  -0.7241       0       0       0;
  -0.1806  -0.6862  -1.5963       0       0       0;
       0        0        0  -0.2400       0       0;
       0        0        0       0  -0.1980       0;
       0        0        0       0       0  -0.1900];
```

The values of coefficients of PID as per section 4.2 are diagonal matrices as given below.

$K_{\infty P} = (0)$,

$K_{\infty I} = diag([-10000, -12000, -8000, -2000, -2000, -1000])$,

$K_{\infty D} = diag([-110, -200, -20, -20, -20, -20])$.

The performance of individual controls has not been observed to be satisfactory except that of PID which alone can accommodate the faults. Other controls namely LQR, H_2, H_∞ or H_∞-OPFB have shown steady state error (as shown in Figure 5). Each of these controls has been augmented with only the integral and derivative components of PID as a hybrid control. The hybrid control has yielded satisfactory results. It may be noted that the aim of the manipulated arm is to reach the target point precisely. Therefore, a performance error index (PEI) has been defined as given in Equation 16.

$$PEI = \sqrt{\sum e_i^2}, \quad for\ i = 1,6 \tag{16}$$

The relative performance is observed for a defined position of the end effectors (trajectory) using different hybrid controls and is presented in Table 2. It may be observed (in Figure 7 and Table-2) that the lowest errors are achieved using H_2 control augmented with PID in all three cases of faults (described in Section 3). The omission of P component as part of the augmented PID helps improving quicker numerical convergence thus improves efficiency of the control system. As depicted in Figure 3, there is large variability in the dynamic parameters which is reflected in the computed (norm of) control gains. Therefore, an offline design of the proposed hybrid control is computationally cost effective whose online implementation has yielded satisfactory control of the robot even under faulty actuator conditions.

Table 2 Performance of Hybrid Control Techniques (Performance Error Index)

Control Strategy	Position Error Index (rms)		
	Case-1	Case-2	Case-3
PID	0.020	0.021	0.020
PID + LQR	0.064	0.061	0.055
PID + H_2 control	0.049	0.047	0.047
PID + H_∞ control	0.046	0.046	0.046
PID + H_∞-SOPF	0.046	0.046	0.046

The performance of these hybrid control techniques in terms of the relative simulation time with reference to the time taken in simulation for the case -3 (under PID + H_2 control as unity), has been obtained as shown in Table 3.

Table 3 Performance of Hybrid Control Techniques (Relative Simulation Time)

Control Strategy	Relative Simulation Time		
	Case-1	Case-2	Case-3
PID	2.62	2.66	2.65
PID + LQR	1.20	1.22	1.15
PID + H_2 control	1.09	1.09	1.00
PID + H_∞ control	1.09	1.10	1.07
PID + H_∞-SOPF	1.09	1.10	1.07

It may be observed in Figure 7, that the total time of simulation is shown as 10 seconds which was a chosen value and does not reflects on the actual time taken by the robot system which is much smaller in magnitude. The simulation results for the accommodation schemes implemented for the simulated fault cases highlight that the tracking errors asymptotically reaches zero for the end position of the robot. The suggested hybrid approach of H_2 control augmented with the integral and derivative components of PID is indeed faster in implementation on a robotic faulty environment.

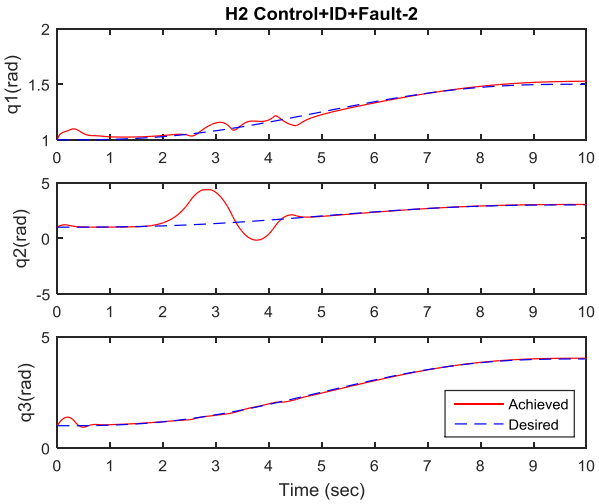

Figure 7A Hybrid control (H_2 and ID) under fault at $q_{1\text{-}3}$ (Fault Case-2)

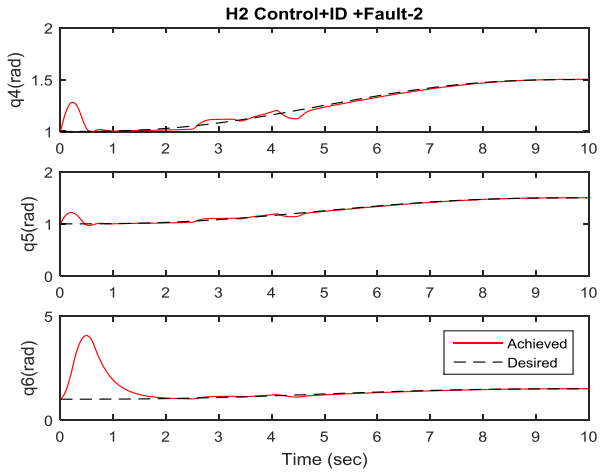

Figure 7B Hybrid control (H_2 and ID) under fault at $q_{4\text{-}6}$ (Fault Case-2)

Conclusions

A hybrid control framework has been proposed for controlling a standard robot arm which has optimal or robust control and PID as an augmented control. The main control utilizes the control gains from an offline linearized model of the PUMA 560 robot. The main control can be based on any of the LQR, H_2, H_∞ or H_∞-OPFB control. The control gains have been obtained offline using equivalent linearization of the robot dynamic system and implemented online on PUMA 560 robot successfully. Based on the relative performance of achieving target position, it has been observed that a hybrid approach offers an efficient fault tolerant control and the most efficient combination has been found to be H_2 control augmented with PID control even in presence of uncertain actuator failure represented by exponential function, sudden or abrupt in nature.

Acknowledgement

The first author acknowledges the kind support provided by Dr. R.K. Agarwal, Director and Dr. P.K. Chopra, HOD, ECE at Ajay Kumar Garg Engg. College, Ghaziabad and Dr. Tasleem Burney, Ph.D. Coordinator at Al Falah University, Dhauj, India.

References

Acosta, L., G.N Marichal,L. Moreno,J,J Rodrigo, A. Hamilton, J.A Mendez (1999). A robotic system based on neural network controllers. *Artificial Intelligence in Eng.* Vol. 13, pp. 393-398.

Clover CL. (1996). Control system design for robots used in simulating dynamic force and moment interaction in virtual reality applications. *Retrospective Theses and Dissertations*, Iowa State University, Paper No. 11141.

Corke P, (2011). *Robotics, Vision & Control*, Springer, ISBN 978-3-642-20143-1.

Corke, PI and Armstrong-Helouvry B. (1994). Search for consensus among model parameters reported for the PUMA 560 robot, *Proc. of the IEEE International Conference on Robotics and Automation,* Vol. 2, pp. 1608–1613.

Doyle, J.C., K. Glover, P. Khargonekar, and B. Francis, (1989). State-space solutions to standard H_2 and H_∞ control problems, *IEEE Transactions on Automatic Control,* vol. 34, no. 8, pp. 831–847.

Gadewadikar J, Lewis FL, Subbarao K, Peng K, Chen BM.(2009). H-infinity static output- feedback control for rotorcraft, *J. Intell Robot Syt*, Vol. 54, Pp. 629-646.

Gahinet, P. and P. Apkarian, (1994). A linear matrix inequality approach to H_∞-control, *Int J. Robust and Nonlinear Control*, Vol. 4(4), Pp. 421–448.

Gao Z, Cecati C, Ding SX. (2015). A survey of fault diagnosis and fault-tolerant techniques- Part II: Fault diagnosis with knowledge based and Hybrid/ active approaches. *IEEE Transaction on Industrial Electronics*, Vol. 62(6), Pp. 3768-3774.

Hossam N. D. (2014). Robust Tracking Control for Flexible Joint Robot Manipulators Using Variable Structure Compensator. *International Journal of Current Engineering and Technology*, Vol.4, No.2 , Pp. 1110-1116.

Jerry Rutherford, Using The PUMA 560 Robot . http://rutherford-robotics.com/puma/using% 20the % 20puma%20robot.pdf. Date accessed: 01/09/2015.

Lei SY and Meng Joo, (2004). Hybrid fuzzy control of robotics systems. *IEEE Transactions on Fuzzy Systems, Vol.* 12, Pp. 755-765.

Levi,I, Berman,N and Ailon, A. (2007). Robust Adaptive Nonlinear H∞ Control for Robot Manipulators. *Proc. Mediterranean Conference on control and Automation*, Athens, Paper No. T31-028.

Lotfi C., Philippe P., Francois P. and Cedric Baradat (2010). A mixed GPC-H∞ robust cascade position-pressure control strategy for electro-pneumatic cylinders. *IEEE International Conference on Robotics and Automation*, Anchorage, Alaska, USA, Pp. 5147-5154.

Meena,Ruby and Senthil Kumar. (2015). Design of GA Tuned Two-degree Freedom of PID Controller for an Interconnected Three Area Automatic Generation Control System, *Indian Journal of Science and Technology,* Vol 8(12).

Mittal,Seema, Dave,MP and KumarAnil, (2016). Comparison of Techniques for Disturbance-Tolerant Position Control of the Manipulator of *PUMA* Robot using PID, *Indian Journal of Science and Technology* (under review).

Ogata Katsuhiko. *Modern Control Engineering*. Fifth Edition, 2012. PHI/Pearson.

Pawar, Suraj Deelip (2016). Performance of Induction Motor by Indirect Vector Controlled Method using PI and Fuzzy Controller. *International Journal of Current Engineering and Technology*, Vol. 6, No. 3 , Pp. 1045-1048.

Rugthum T, Tao G. (2015). An adaptive actuator failure compensation scheme for a cooperative manipulator system with parameter uncertainties. *IEEE 54th Annual Conference on Decision and Control*, Osaka, Japan, Pp. 6282-6287.

Sunan N. Huang & Kok Kiang Tan (2008). Fault Detection, Isolation & accommodation Control in Robotic Systems. *IEEE Transactions on Automation*, Vol. 5, No. 3. Pp. 480-489.

Tihomir Z, Josip K, Mario,E, Branko N and Zeljko S, (2012). Performance Comparison of Different Control Algorithms for Robot Manipulators. *Journal Strojarstvo,* Vol. 54(5), Pp. 399-407 (ISSN 0562-1887).

Vemuri, Arun T. Marios M. Polycarpou (1997). Neural-Network-Based Robust Fault Diagnosis in Robotic Systems. *IEEE Transactions on Neural networks*, Vol. 8, No. 6. Pp. 1410-1420.

Yan D, Lu Y. and Levy D (2015). Parameter Identification of Robot Manipulators: A Heuristic Particle Swarm Search Approach. *PLoS ONE* 10(6):e0129157. doi:10.1371/journal. pone. 0129157.

Zhou K. (1992). On the parameterization of H_∞ controllers. *IEEE Trans. Automatic Control*, Vol. 37(9), Pp. 1442-1445.